N69-11535
nasa TMX-63392

X-612-68-448

EXPLORER 12 MAGNETOPAUSE OBSERVATIONS: LARGE SCALE NON-UNIFORM MOTION

CASE FILE COPY

RICHARD L. KAUFMANN
ANDREI KONRADI

NOVEMBER 1968

GODDARD SPACE FLIGHT CENTER
GREENBELT, MARYLAND

EXPLORER 12 MAGNETOPAUSE OBSERVATIONS:
LARGE SCALE NON-UNIFORM MOTION

Richard L. Kaufmann
Department of Physics
University of New Hampshire
Durham, New Hampshire 03824

and

Andrei Konradi
Goddard Space Flight Center
Greenbelt, Maryland 20771

ABSTRACT

A number of events have been studied which involve brief re-entries of Explorer 12 into the magnetosphere when the satellite appears to be located well beyond the equilibrium magnetopause position. The inverse behavior involving brief emergences of the satellite from the magnetosphere when the satellite appears to be located well below the equilibrium magnetopause position has also been investigated. The events studied provide evidence that relatively small portions of the magnetosphere occasionally become severely distorted. Several possible models of this distortion are discussed. It is concluded that a bump or a wave-like structure appears on the magnetopause. Those structures producing the largest distortions are generally elongated in the north-south direction, and in most cases, the magnetosheath magnetic field is either nearly parallel or nearly anti-parallel to the magnetospheric field. As a result, the distortions do not involve severe bending of any magnetic field lines. The distortion frequently appears to be triggered by a change in the properties of the solar wind.

Data Presentation. Multiple crossings of the magnetopause are common. Such events have been identified in data from charged particle and magnetic field detectors carried aboard nearly every satellite which has penetrated the magnetopause. The present work deals with a certain set of these multiple crossings, a set which provides evidence for non-uniform motion of the magnetopause.

The magnetopause can usually be located with Explorer 12 data using either the magnetometer (Cahill and Amazeen, 1963) or the ion and electron detector (Davis and Williamson, 1963). Several examples of typical magnetopause crossings as seen by these detectors have been given previously (Konradi and Kaufmann, 1965).

Explorer 12 penetrated the magnetopause between 06:00 and 13:00 local time at radial distances between 7.8 earth radii and apogee of 13.1 earth radii. Multiple boundary crossings seen by Explorer 12 in this region usually involve one or more re-entries into the magnetosphere which are separated by time intervals of only a few minutes (Hyde, 1967). Figure 1, which is reproduced from the work of Hyde (1967), shows that most multiple boundary crossings are separated by less than 15 to 20 minutes. The lack of crossings separated by less than two minutes is produced by data sampling. Anderson et al. (1968) have presented similar results using IMP satellite data. This similarity indicates that the shape of Figure 1 is not sensitively dependent upon the detectors used, the satellite orbit, or the time interval during which data were collected. We shall term boundary crossings separated by less than 15 minutes "ordinary multiple boundary events". Such observations are consistent with the assumption that the magnetopause oscillates uniformly in and out over distances on the order of 0.1 earth radii and with periods of a few minutes. It is also consistent with the assumption that waves are continuously present on the magnetopause and therefore produce nearly continuous local expansions and contractions of the magnetosphere. Such uniform motion of the magnetopause produces multiple boundary crossings in which the satellite spends roughly equal time intervals inside and outside the magnetosphere, as illustrated in Figure 2a.

Figure 1 also shows a rather flat distribution of events separated by periods exceeding 15 minutes. These are the events which will be treated in the present work, and will be termed "re-entry events". Finally, the re-entry events must be subdivided into three classes in order to separate events produced by physically different processes.

A "brief re-entry event" is defined to involve the following sequence of observations: the satellite is first in the magnetosheath for at least 15 minutes, then enters the magnetosphere for not more than 15 minutes, and finally returns to the magnetosheath for at least 15 minutes. Times for magnetopause crossings are determined from magnetometer data. The magnetic field direction and magnitude, and the fluxes of electrons above about 20 kev and of protons above about 140 kev must all return to near magnetospheric levels in all re-entry events. Finally, to classify as a brief re-entry, we require at least one magnetopause boundary crossing to appear at a radial distance of less than 12 earth radii on the inbound and outbound portions of the orbit. This requirement is introduced to eliminate multiple boundary crossings seen when the satellite is moving very slowly near apogee, since these could be produced by small scale motions of the magnetopause. The satellite radial velocity is 0.4 km/sec at 12 earth radii and reaches 1.1 km/sec at 8 earth radii.

Events satisfying the above criteria except that the duration of the re-entry exceeds 15 minutes are called "ordinary re-entry events".

Examples of brief re-entry events are shown in Figures 3 to 5. Figure 3 illustrates a single magnetopause crossing at 04:15. At 06:08 energetic electrons are again detected but the magnetic field does not return to its magnetospheric value. This is not a re-entry event. At 07:35 energetic electrons are seen once more and the field direction does return to near its magnetospheric value. The field magnitude rises somewhat, not to the level seen well within the magnetosphere but to approximately the level one would expect if the magnetosphere were to expand outward by 2 1/2 earth radii to envelop the satellite. The most striking property of this and other brief re-entry events is its short duration relative to its separation from other magnetopause crossings.

Figure 4 is an extension of the same orbit shown in Figure 3. At 14:46, approximately 7 hours after the brief re-entry event in Figure 3, another event is seen. Finally, at 17:32, a third event of this type occurs.

Figure 5 shows the inbound pass of September 2 during which brief re-entry events were seen at 07:46 and 12:03. An ordinary multiple boundary crossing is also seen on this pass slightly after 14:00. Here the satellite enters the magnetosphere for 2 minutes, leaves for 6 minutes, and then re-enters for a longer period.

Brief re-entry events are not consistent with a picture of uniform boundary motion as illustrated in Figure 2a. Figure 2b illustrates a type of non-uniform variation in radial distance to the magnetopause that is consistent with these observations. Note that we do not require the entire magnetopause to undergo the rapid motion implied by Figure 2b. It is sufficient for the rapid motion to be localized to a small region of the magnetopause.

Figures 4 and 5 also contain several examples of what appears to be the inverse of a brief re-entry event. At 18:57 on September 25 and at 14:36 and 15:25 on September 2 the satellite leaves the magnetosphere for a few minutes after having been inside for more than 15 minutes. Events of this type will be called "brief emergence events".

The selection criteria are the same as for the brief re-entry events except the satellite must first be in the magnetosphere for at least 15 minutes, then leave for less than 15 minutes, and finally re-enter the magnetosphere for at least 15 minutes.

Figures 3 to 5 illustrate the short duration of the events being studied but do not show them in sufficient detail to make identification positive. Each event has been examined in detail. Figures 6 to 8 provide examples. All available magnetometer data and data from the most frequently sampled ion and electron detector energy channel have been used in preparing these figures. Each magnetic field point represents the average of 16 vector measurements taken during a five-second period. Each particle flux point is the maximum flux scanned by the spinning detector during a 5-second interval (satellite spin period is 2 seconds).

The re-entry shown in Figure 6 is similar to most ordinary traversals of the magnetopause. The field direction changes suddenly to the magnetospheric values shown in Figure 5 (α = 100°, ψ = 110°). The magnitude increases suddenly, and both magnitude and direction remain steady druing the event. The standard deviation in field magnitude is about 4 gammas during most of the interval shown, and can be attributed entirely to data digitization (Kaufmann, 1967). A fairly steady energetic particle flux is seen within the high field region.

Pitch angle distributions of the trapped particles have also been calculated, and are usually similar to ordinary magnetospheric pitch angle distributions. For example, data from the event beginning at 17:32 on September 25 have previously been described in detail (Konradi and Kaufmann, 1965). Nearly all the events that have been detected are similar to the one shown in Figure 6.

Figure 7 is an example of one of the few unusual events. The field direction again changes abruptly to the magnetospheric values shown in Figure 3 ($\alpha = 60°$, $\psi = 60°$) as energetic particles are first seen. The field magnitude increases at this point, but the field magnitude and direction and the particle fluxes fluctuate more than is typical within the magnetosphere.

Figure 8 shows a brief emergence event. The small increase in field magnitude just before the event is present in several cases, and suggests the magnetosphere is being compressed just prior to the observed boundary penetration.

Important characteristics of each event studied in this work are summarized in Table I.

Event Selection Criteria. Even if the magnetopause only underwent uniform oscillatory motion, some events meeting the criteria stated above would be found. In this section we will show that the number of events found is not sensitively dependent on the selection criteria and that brief re-entry events occur much more frequently than they would if the magnetopause oscillated uniformly.

The short duration of most re-entry events is most striking if we examine those cases in which the satellite has been in the magnetosheath for a period of at least two hours before and after the event. If the magnetopause moved uniformly in and out as in Figure 2a, one would expect most of these re-entries to last for periods of about two hours. Seven events in this class were seen, and the average duration of these re-entry events was less than 6 minutes. Every time the magnetosphere expanded enough to envelop the satellite when the satellite appeared to be more than 2 hours (about 1 earth radius) within the magnetosheath, the resulting envelopment lasted less than 15 minutes. It is clear that the magnetopause does not oscillate uniformly in and out over distances on the order of one earth radius with periods on the order of one or two hours.

Emergence events show a similar tendency to be brief. Seven events have been detected which fall into this class. The average duration of all seven events is three minutes.

Finally, re-entry and emergence events could be classified as brief by examining the ratio of the time from the nearest magnetopause crossing to the duration of the event. Uniform boundary motion, as illustrated in Figure 2a, should produce a ratio near one. Non-uniform motion (Figure 2b) should produce either large or small ratios. Figure 9 presents this ratio for all observed re-entry events. The tendency for this ratio to be very large or very small is most evident for the circled points, which are separated by more than one hour from the next magnetopause crossing.

Events could have been separated into exactly the same groups by specifying this ratio rather than by using the previously stated criteria. The fact that the events of interest could be selected by either of two quite different methods indicates that the selection process is not sensitively dependent on the specific criteria which have been used.

Some model must be introduced to show quantitatively that we are not simply observing those few brief events that would be expected as the satellite happens to pass through the extreme outer edge of one of the uniform excursions illustrated in Figure 2a.

The simplest model involves a stationary satellite with the magnetopause expanding and contracting sinusoidally. The radial distance to the magnetopause is

$$R = R_o + \Delta R \cos \pi t \qquad (1)$$

where R_o is the equilibrium radial distance and ΔR is the oscillation amplitude. The probability that a satellite placed at random in the range $(R_o - \Delta R, R_o + \Delta R)$ is located below a point R_1 is, using equation (1)

$$P = \frac{R_1 - R_o + \Delta R}{2\Delta R} = \frac{1 + \cos \pi t_1}{2} \qquad (2)$$

The ratio of the time this stationary satellite spends within the magnetosphere to the time spend outside the magnetosphere is then

$$f = t_1/(1-t_1) \qquad (3)$$

The probability that a satellite will be located at a radial distance such that it spends less than the ratio of times, f, inside the magnetosphere is, from equations (2) and (3)

$$P = \frac{1}{2} + \frac{1}{2} \cos\left(\frac{\pi f}{1+f}\right) \quad (4)$$

This expression predicts that the ratio f (the abscissa of Figure 9 is 1/f) would be less than 0.1 in only 2% of all the re-entries. By symmetry, the ratio would also be greater than 10 in 2% of the cases. We actually see more than 10 times too many events with ratios exceeding these limits to be explained by this simple model. The discrepancy is even more pronounced for ratios exceeding 20 and 50. Here there are, respectively, more than 30 and more than 100 times too many events to be accounted for by uniform boundary motion. We conclude that of the 22 events studied in this paper, one or two are probably the result of uniform oscillatory motion of the magnetopause.

Models of Non-uniform Motion. Five possible types of non-uniform boundary motion are shown in Figure 10. Figure 10a illustrates the possibility that the entire magnetopause rapidly expands and contracts without being greatly distorted. This motion could be in response to a fairly rapid (5 to 15 minute) change in solar wind pressure.

Figure 10b shows the magnetopause being pushed in at one point and simultaneously bulging out elsewhere. Such a distortion would be expected if a small (<10 earth radii) inhomogeneous region in the solar wind were to strike the magnetopause. A similar distortion could be produced by a thin discontinuity in the solar wind as it sweeps past the magnetosphere.

The possibility that a large amplitude wave propagates around the magnetopause is illustrated in Figure 10c. Models b and c are quite similar. A brief re-entry event, for example, would represent the period during which the bulge in Figure 10b or the wave in Figure 10c envelops the satellite.

An extreme example of what could happen if a very large amplitude wave were to form is shown in Figure 10d. Here the wave has completely detached from the magnetosphere. This results in a flux tube containing magnetospheric field lines and magnetospheric plasma which is imbedded in and swept along with the solar plasma. A brief re-entry event could be produced as the flux tube was swept past the satellite.

Figure 10e shows a transition between an open and a closed magnetosphere and is intended to represent any basic change in magnetopause structure. The particular transition illustrated has been discussed by Sonnerup (1965), and involves the creation or annihilation of neutral points or lines. While the magnetosphere is opening or closing, there must be a line on the magnetosheath which separates the open from the closed portions. This line then moves as one region grows and the other shrinks until the magnetosphere is completely open or closed. The propagation of this line could distort the magnetopause as shown in Figures 10b or c. The principal distinction between Figures 10b, c, and e is the cause of the wave-like perturbation or bulge. It could be produced: as a direct response to a small scale or localized change in the incident solar plasma, as a response to the passage of a thin, large scale discontinuity separating two significantly different regions of solar plasma, or as an indirect response to some change in the solar plasma. The indirect response could involve an instability of the magnetopause (Sen, 1965, Anderson et al., 1968) or a basic change in magnetospheric topology (Sonnerup, 1965).

Ground Magnetograms. Ground magnetograms can aid in distinguishing between some of the above models. If the entire boundary were compressed and then expanded several minutes later (Model a), a bump would be seen in equatorial magnetograms. To account for the observations the compression and expansion would have to be at least 0.2 to 2.5 earth radii (Table I) and to average at least one earth radius. Sudden impulses would be produced by changes in the magnetopause current layer and by any changes in the energy of trapped particles which may take place during the event. The amplitudes of sudden impulses produced by changes in magnetopause currents can be estimated using Mead's (1964) model. They vary between about 1 and 20 gammas for the observed events, and average 10 gammas. The few events which would produce sudden impulses of less than 5 gammas could be missed in ground magnetograms, but larger events should be seen. Only one event was accompanied by an observable perturbation in equatorial magnetograms. This one event, the 09:56 August 27 brief emergence, is discussed in a later section of this paper. From the nearly complete lack of magnetic field perturbations at equatorial stations, we conclude that most of the events studied in this paper are not produced by impulsive expansions or contractions of the entire magnetopause.

All the other models (Figures 9b-e) involve distortions of magnetic field lines. These distortions should propagate down field lines and be observed in auroral zone magnetograms. A number of auroral magnetograms were scanned with inconclusive results. One difficulty is that magnetograms at these stations are frequently distrubed so that even a 20 gamma perturbation would often be lost in the noise produced by ionospheric currents. Several of the events studied were closely associated with the commencement of large micropulsation events (damped waves with periods of several minutes). The micropulsation events, however, are much more common than the brief re-entry and emergence events. In addition, a number of brief re-entry and emergence events were not associated with micropulsations. These observations suggest that giant micropulsations may be produced by distortions in the magnetopause, but much smaller distortions than those studied here must be responsible for many of them.

Ground magnetograms, therefore, can eliminate model a but were not able to distinguish between the other models.

Boundary Normal. Magnetic field measurements have been used to determine the direction of the magnetopause normal vector, as described by Sonnerup and Cahill (1967).

Determination of this direction provides a test for several of the proposed models. If a wave or bump is formed, interactions with the solar wind should cause it to propagate from the subsolar point toward the tail of the magnetosphere. We would then expect the magnetopause normal to tip toward the tail or anti-sun direction each time the satellite enters the magnetosphere and to tip toward the sun each time the satellite enters the magnetosheath (Figure 10b, c). If waves are produced by an instability they should grow as they propagate toward the tail, so distortions should become more severe as the distance from the subsolar point increases. Completely detached flux tubes (Figure 10d) would exhibit normal vectors which deviate markedly from the direction predicted by steady state theoretical models, at least when projected onto the equatorial plane.

In order to provide confidence in the results of magnetopause normal calculations, data from each passage through the magnetopause have been analyzed in ten separate ways using the methods of Sonnerup and Cahill (1967). For each passage, a section of data was selected which included the principal magnetic field direction and magnitude changes and which extended from a point the satellite was clearly within the magnetosheath to a point the satellite was clearly within the magnetosphere. Individual data points taken three times per second were then used to calculate a boundary normal. The standard deviation of these individual data points is about 10 gammas. The data were then divided into two segments, using the center of the magnetopause as the dividing line, and these segments were analyzed to determine boundary normals. Next, a segment of data containing only the central portion of the magnetopause where gradients are steepest was similarly analyzed.

The individual data points were then vectorially averaged in groups of 6 or 7. The number of points used in each group was selected so that each group contained data from one complete satellite revolution, thereby minimizing any possible modulation at the satellite spin period. These averaged data were divided into four segments as described above and used as inputs to the normal vector calculations. The averaged inputs, then, consisted of fewer data points, but each point had a standard deviation of only about 4 gammas. Finally, all individual data points were averaged in groups of 4 and 16 and used as inputs to provide the last 2 estimates of the boundary normal.

The reason for calculating boundary normals in so many ways for each data segment is that the calculations are inefficient at providing reliable results. The normal is assumed to point in the direction in which the standard deviation of the magnetic field measurements is a minimum. In some cases, however, the minimum standard deviation is along the satellite spin axis since one magnetometer sensor points in this direction and may remain in one digitization level for an appreciable time interval. All results in which the calculated normal vector was within 45° of the satellite spin axis were considered unreliable. The spin axis was nearly tangent to the theoretical magnetopause (Mead and Beard, 1965), so that theoretical normal vectors were never within 45° of the spin axis. In a few cases the set of ten calculations yielded several normal vectors which were not along the spin axis and were also not consitent with each other. These results are presented in Figures 11 and 12. The solid points represent normal directions which were determined consistently in at least five of the ten analyses. Open points were determined consistently in three or four of the ten analyses. To be consistent, each calculated boundary normal was required to deviate from the average direction shown in Figures 11 and 12 by less than 20° when projected onto the equatorial plane and when projected onto a meridian plane.

The north-south deviations of the calculated boundary normals from the radial direction are plotted as a function of the geomagnetic latitude of the sun in Figure 11. The data are compared to a fit to Spreiter and Summer's (1963) observations of the tip during normal magnetopause crossings based on Explorer 12 data. The theoretical model appears to underestimate the distortion of the magnetosphere when the sun is not perpendicular to the earth's dipole axis. Sonnerup and Cahill's fit, however, is in reasonable agreement with the present data and, except for the two points in parentheses, the scatter in the data is essentially the same as that seen during ordinary magnetopause crossings. This indicates that even during periods when the magnetopause must be moving rapidly, the normal vector does not tip significantly in the north-sourth direction. Individual magnetic field lines, therefore, are not being distorted significantly more during the events studied here than they are on a typical day.

The eastward tip of the magnetopause normal vector relative to Mead and Beard's (1964) theoretical model is plotted as a function of geomagnetic local time in Figure 12. At geomagnetic local times later than 10:00, the points are scattered slightly more than similar points determined by Sonnerup and Cahill (1967, 1968) using ordinary boundary traversal data. The fact that the average calculated boundary normal tips about 10° westward of the theoretical boundary normal in this local time interval is probably not significant. Uncertainties in the spin axis direction and magnetometer errors at these low field strengths produce a 10° uncertainty in the absolute direction of magnetic field measurements.

In this geomagnetic local time interval, the directions obtained as the satellite leaves the magnetosphere (labelled by the letter L) are displaced an average of about 10° to the east of the directions obtained as the satellite enters the magnetosphere (labelled by the letter E). This displacement is consistent with the picture of either a wave or a bump on the magnetopause propagating from the subsolar point to the tail along the dawn side of the magnetosphere, as discussed earlier in connection with Figure 10.

At earlier geomagnetic local times, much larger deviations from the theoretical model are observed. The two points in parentheses which showed substantial deviations in the north-south direction also show substantial deviations in the east-west direction. These two points were obtained during the same brief re-entry event, and their reliability is marginal since each just barely met our requirement of deviating more than 45° from the satellite's spin axis. Note that two of the solid points, which are considered most reliable, deviate by 50° from the theoretical boundary normal in the east-west direction. These results indicate that severe distortions of the magnetopause occasionally take place at angles of more than 30° from the earth-sun line. Sonnerup and Cahill (1968) also found similar, occasional deviations in this same region. The results are even consistent with Figure 10d which shows flux tubes completely separated from the magnetosphere. The few normal vector directions observed before 10:00 in Figure 12 are generally perpendicular to the earth-sun line, implying that if these separated flux tubes exist, they are elongated along the earth-sun line. It is, of course, also possible that flux tubes do not separate from the magnetosphere. We would then require the magnetopause to be strongly distorted from its usual configuration. The observed boundary normal for these few events is generally in the direction one would expect to see far back in the tail of the magnetosphere.

Sample Events. Data from a few events which can most clearly be interpreted in terms of the models presented in Figure 10 will be discussed here. None of the observed events provided any indication that the entire day side of the magnetosphere suddenly expands and then contracts several minutes later without substantial deformation (Figure 10a). The only event which was accompanied by a bump on equatorial magnetograms was the brief emergence of August 27. Ground observations are summarized in Figure 13. The event was seen throughout the dawn hemisphere but not in the dusk hemisphere. The amplitude of the H-component of the disturbance, as seen at ground stations, is shown on Figure 13. The variation of amplitude with geomagnetic latitude of the observer indicates that the disturbance was not a pure compressional hydromagnetic wave produced by uniform boundary compression. On the contrary, the large amplitude disturbances seen at high latitudes indicate the presence of hydromagnetic disturbances traveling along field lines, and their corresponding ionospheric currents.

Satellite magnetometer data also show that, though the field magnitude does not change significantly, the direction of the field within the magnetosphere changes suddenly by about 15° coincident with the brief emergence event. Most of this change is in the inclination angle. The theoretical inclination at the satellite location for the Jensen and Cain (1962) field model is -36°. The observed inclination is -16° before the event and -3° after the event. These results indicate that the magnetosphere was compressed relative to a dipole field before the brief emergence event, much as it usually is (Mead and Cahill, 1967). After the event, the field distortion indicates substantial additional compression relative to a dipole configuration.

This event was observed on seven rapid run magnetograms. The peak of the disturbance in the H-component magnetograms occurred between 0 and 5 minutes after the mid-point of the event as seen on the satellite. The delay times to the peaks do not appear to be simply correlated with either the geomagnetic latitude or longitude of the observation point. No perturbation in the satellite record was observed before 09:56 while the disturbance began on two ground magnetograms one or two minutes earlier. This indicates that the portion of the magnetopause near the satellite was not the first to be perturbed. No disturbance was seen on any rapid run magnetogram before 09:54 or after 10:07, providing some limit to the duration of the perturbation.

The magnetic field at the satellite rose about 10 gammas during the minute before entering the magnetosheath. This behavior is similar to that shown in Figure 8 for the 14:36, September 2 event. Similar observations were also made near several other brief emergence events. If a large portion of the magnetosphere were being compressed as the region near the satellite is, a 10 gamma compressional hydromagnetic wave would be produced and should be seen at equatorial stations. The fact that field compression is observed at the satellite during several events, but is seen only once at equatorial ground stations again indicates that only a small portion of the magnetosphere is being compressed at any given time.

The energetic particle fluxes and pitch angle distributions before and after the August 27 event are typical of those usually seen within the magnetosphere.

Figure 14 illustrates the time development of one possible magnetopause distortion which could produce the August 27 brief emergence event. Figure 14a shows the magnetopause just before the arrival of a tangential discontinuity which is aligned at the garden hose angle. This discontinuity separates a low density region of interplanetary plasma from a high density region.

In Figure 14b the discontinuity has advanced so that a portion of the magnetopause is in contact with the high density plasma. This portion of the magnetopause is shown compressed from its original equilibrium configuration. This figure also shows a portion of the magnetopause which has expanded beyond its original equilibrium configuration to form a bulge. Such an expansion is expected to occur when the fast (compressional) magnetosonic wave velocity inside the magnetosphere exceeds the solar wind velocity. When this condition arises, the enhanced pressure is transmitted within the magnetosphere to the inside of the magnetopause before the high density solar plasma has arrived outside the magnetopause to balance this enhanced pressure.

The effect should be more pronounced in the dawn hemisphere when the discontinuity is aligned as shown in Figure 14. The velocity of the line of intersection between a plane discontinuity and the magnetopause is $v = v_n/\cos\theta$, where v_n is the propagation speed of the plane discontinuity normal to its surface, and θ is the angle between the discontinuity normal vector and the magnetopause normal. The velocity that a plane interface sweeps along the magnetopause is a minimum several hours before local noon where the two normal vectors are nearly perpendicular. It is here that the bulge shown in Figure 14 would be most likely to form.

A brief emergence event would be produced if the magnetopause overshoots its new equilibrium position. The particle density within the thin tangential discontinuity is generally higher than in the bulk of the high density plasma. This effect results from the continuity of the total (magnetic plus gas) pressure, $(B^2/8\pi) + p$, through the discontinuity. The magnetic field magnitude reaches a minimum within a tangential discontinuity, so the particle pressure must reach a maximum.

The inverse of Figure 14, obtained by interchanging the high- and low-density regions, could produce an indentation in the magnetopause rather than a bulge. Such an indentation would also produce a brief emergence event.

The distortion of the plane discontinuity by the earth's bow shock has been omitted from Figure 14. This does not alter the basic conclusion that any thin discontinuity, whether plane or curved, will interact first with some one region of the magnetopause and will then sweep to other regions. In fact a shock wave or any other sharply bounded inhomogeneity in the solar wind could produce a sudden large scale distortion of the magnetopause. A shock wave, for example, would probably be aligned so that its normal vector would be roughly radial from the sun. Such a discontinuity would be most likely to produce bulges well away from the earth-sun line, for it is here that the discontinuity and magnetopause normals are most nearly perpendicular.

Figure 5 shows that some basic change took place in the magnetosheath field during each of the brief re-entry events on September 2. The field was much quieter between events that it was before the 07:46 event or after the 12:03 event. This, again, suggests that the associated magnetopause distortions were initiated by some change in the solar wind. The 10 gamma rise in magnetic field magnitude starting at 07:53 in Figure 6 suggests that shortly after having expanded to envelop the satellite, the magnetopause is being compressed by increased solar wind pressure. The fact that a 10 gamma sudden impulse does not appear in equatorial magnetograms again shows that the expansion and compression are localized. A similar 10-gamma magnitude peak was previously noted just before the 14:36 brief emergence event (Figure 8) and a similar 20-gamma peak also preceded the 15:25 brief emergence event.

Figures 5, 6, and 8 also show that the magnetic field in the magnetosheath was roughly anti-parallel to the earth's field on September 2. Most of the events studied (See Table I) involved angle changes near 180°, as on September 2, or near 0° as on October 30 (Figure 15). This fact is also consistent with our conclusion that the magnetopause is being severely distorted in localized regions. It is energetically much easier to distort a region of the magnetopause when the field in the magnetosheath is parallel or anti-parallel to the magnetospheric field in that region. Coupled with the observation that most distortions of the magnetopause normal vector involve deviations in the east-west direction (Figures 11 and 12), we conclude that large scale distortions of the magnetopause usually do not involve severe bending of field lines either in the magnetosphere or in the magnetosheath.

Topology Changes. Figure 10e illustrates the possibility that a bulge or indentation could be produced in the magnetosphere as a neutral line propagates along the magnetopause. The neutral line separates a closed portion of the magnetosphere from an open portion. By open, we refer to a region in which the earth's magnetic field lines become directly connected to interplanetary field lines, as suggested by Dungey (1961).

Preliminary studies of a few events have revealed magnetic field and energetic particle flux changes which are consistent with the possibility of a basic topological change. A great deal of additional analysis will, however, be required before any definite statements concerning the necessity of such topological changes can be made.

ACKNOWLEDGEMENTS

We wish to express our appreciation to Dr. L. J. Cahill, Jr. and L. R. Davis for the use of their data and for many helpful discussions. It is also a pleasure to acknowledge the assistance of B. U. Ö. Sonnerup, particularly with regard to the magnetopause normal vector calculations.

This work was supported in part by the Atmospheric Sciences Section, NSF Grants GP-5255 and GA-1131.

FIGURE CAPTIONS

Figure 1. The number of times which multiple crossings of the magnetopause were observed is plotted as a function of the time interval between the multiple crossings. From Hyde (1967).

Figure 2. Models of uniform (a) and non-uniform (b) motion of the magnetopause. Shading is added above the time axis when the satellite is inside the magnetosphere.

Figure 3. September 25 outbound orbit. I_8, the ion and electron detector's eighth dynode current, is a measure of the total energy flux of electrons above about 20 kev and protons above about 140 kev. The electron flux above about 20 kev is presented below I_8 using the detector's scatter geometry (Davis and Williamson, 1963). The bottom three curves show the magnetic field magnitude, B, and orientation, α and ψ (Cahill and Amazeen, 1963). Shaded intervals indicate periods when the satellite was inside the magnetosphere.

Figure 4. Continuation of data in Figure 3. September 25 inbound orbit.

Figure 5. September 2 inbound orbit. Similar to Figure 3.

Figure 6. Detail of a brief re-entry event shown in Figure 5. I_8, the ion and electron detector's eighth dynode current, represents the flux of electrons above about 30 kev and protons above about 200 kev.

Figure 7. Detail of a brief re-entry event shown in Figure 3.

Figure 8. Detail of a brief emergence event shown in Figure 5.

Figure 9. Events are separated into three groups by the criteria described in the text. For each event, the ratio of time from nearest magnetopause crossing to the duration of the event is shown. Note the groups do not overlap. Therefore, events can be separated into exactly the same three groups by specifying the ratio defined above.

Figure 10. Five possible models of magnetospheric distortion are sketched.

Figure 11. The northward tip of the measured magnetopause normal vector, δ_n, is plotted as a function of λ, the sun's geomagnetic latitude. The line $\delta_n = 0.18\lambda$ is a fit to Spreiter and Summer's (1963) theoretical model. The line $\delta_n = 0.64\ \lambda - 3.3$ is the fit made by Sonnerup and Cahill (1968) using Explorer 12 measurements from single and multiple magnetopause crossings. A letter E or L near a point indicates the satellite was entering or leaving the magnetosphere as the magnetopause normal was being measured. The solid points are considered more reliable than the open points, as discussed in the text.

Figure 12. The difference between the eastward tips of the measured magnetopause normal and the theoretical normal, using Mead and Beard's (1965) model, is plotted as a function of GMLT, the geomagnetic local time at which the observation is made. Other symbols are the same as in Figure 11.

Figure 13. Perturbations in the H-component of ground magnetograms are summarized for the 09:56 August 27 brief emergence event. A symbol is placed at the geomagnetic latitude and geomagnetic local time of each ground station. Numbers give the amplitudes of the disturbance seen at the stations in gammas, while an X means that no significant perturbation could be found. Circled points represent stations in the southern hemisphere. The geomagnetic local time of the satellite is indicated by an arrow.

Figure 14. The magnetospheric distortion expected as a plane tangential discontinuity sweeps past the magnetosphere is sketched in the geomagnetic equatorial plane. Distortions produced when the plane discontinuity passes through the bow shock have been omitted.

Figure 15. Detail of the 02:09 October 30 brief emergence event.

Table I. All events studied are listed. BR and BE signify brief re-entry and brief emergence events. ΔT_B is the time interval by which the event is separated from the next nearest magnetopause crossing, and ΔR_B is the radial distance the satellite has moved during this time interval. ΔT_D is the duration of the event. β's are angles, in degrees, between the field directions just inside the magnetosphere and just inside the magnetosheath. Field data have been averaged over about one minute on either side of the magnetopause to obtain these directions. No values of β are given when the field direction fluctuated markedly during these one-minute intervals. The subscripts E and L label measurements made as the satellite was entering and leaving the magnetosphere.

TABLE I

DATE	TIME	EVENT	ΔT_B(min)	$\Delta R_B (R_E)$	ΔT_D(min)	β_E	β_L
Aug. 22	0018	BR	35	0.35	5		
Aug. 26	0728	BR	25	0.44	2		
Aug. 27	0956	BE	113	1.66	2	20	50
Sept. 2	0746	BR	250	1.12	8		
Sept. 2	1203	BR	120	1.25	1		
Sept. 2	1436	BE	24	0.32	3	130	125
Sept. 2	1525	BE	47	0.69	3	160	150
Sept. 5	1732	BR	211	1.66	15	25	150
Sept.12	1351	BR	27	0.39	2	170	140
Sept.25	0735	BR	198	2.45	8	170	160
Sept.25	1446	BR	163	0.85	2	120	
Sept.25	1732	BR	64	0.53	1	15	25
Sept.25	1857	BE	20	0.22	3	20	20
Sept.30	0659	BE	38	0.52	8	160	165
Sept.30	0746	BE	42	0.62	3	110	160
Oct. 6	1009	BR	76	0.75	9	160	165
Oct. 12	0546	BR	101	0.54	3		
Oct. 12	0730	BR	72	0.58	4		
Oct. 30	0209	BE	340	1.61	1	10	10
Nov. 5	1131	BR	176	1.09	3		
Nov. 7	1448	BR	155	0.92	2		
Nov. 7	1615	BR	85	0.21	13		

REFERENCES

Anderson, K. A., J. H. Binsack, and D. H. Fairfield, Hydromagnetic disturbances of 3- to 15- minute period on the magnetopause and their relation to bow shock spikes, J. Geophys. Res., 73, 2371-2386, 1968.

Cahill, L. J., and P. G. Amazeen, The boundary of the geomagnetic field, J. Geophys. Res., 68, 1835-1843, 1963.

Davis, L. R., and J. M. Williamson, Low energy trapped protons, Space Res., 3, 365-375, 1963.

Dungey, J. W., Interplanetary magnetic field and the auroral zone, Phys. Rev. Letters, 6, 47-48, 1961.

Hyde, R. S., Explorer 12 magnetometer observations of the magnetosphere boundary region, Univ. of New Hampshire Report, UNH-67-6, 1967.

Jensen, D. C., and J. C. Cain, An interim geomagnetic field (Abstract), J. Geophys. Res., 67, 3568, 1962.

Kaufmann, R. L., Shock observations with the Explorer 12 magnetometer, J. Geophys. Res., 72, 2323-2342, 1967.

Konradi, A., and R. L. Kaufmann, Evidence for rapid motion of the outer boundary of the magnetosphere, J. Geophys. Res., 70, 1627-1637, 1965.

Mead, G. D., Deformation of the geomagnetic field by the solar wind, J. Geophys. Res., 69, 1181-1195, 1964.

Mead, G. D., and D. B. Beard, Shape of the geomagnetic field solar wind boundary, J. Geophys. Res., 69, 1169-1179, 1964.

Mead, G. D., and L. J. Cahill, Jr., Explorer 12 measurements of the distortion of the geomagnetic field by the solar wind, J. Geophys. Res., 72, 2737-2748, 1967.

Sen, A. K., Stability of the magnetospheric boundary, Planet. Space Sci., 13, 131-141, 1965.

Sonnerup, B. U. Ö., On the stability of the closed magnetosphere, J. Geophys. Res., 70, 1051-1060, 1965.

Sonnerup, B. U. Ö., and L. J. Cahill, Jr., Magnetopause structure and attitude from Explorer 12 observations, J. Geophys. Res., 72, 171-183, 1967.

Sonnerup, B. U. Ö., and L. J. Cahill, Jr., Explorer 12 observations of the magnetopause current layer, *J. Geophys. Res.*, *73*, 1757-1770, 1968.

Spreiter, J. R., and A. L. Summers, Effect of uniform external pressure and oblique incidence of the solar wind on the terminal shape of the geomagnetic field, *NASA Report R-181*, 1963.

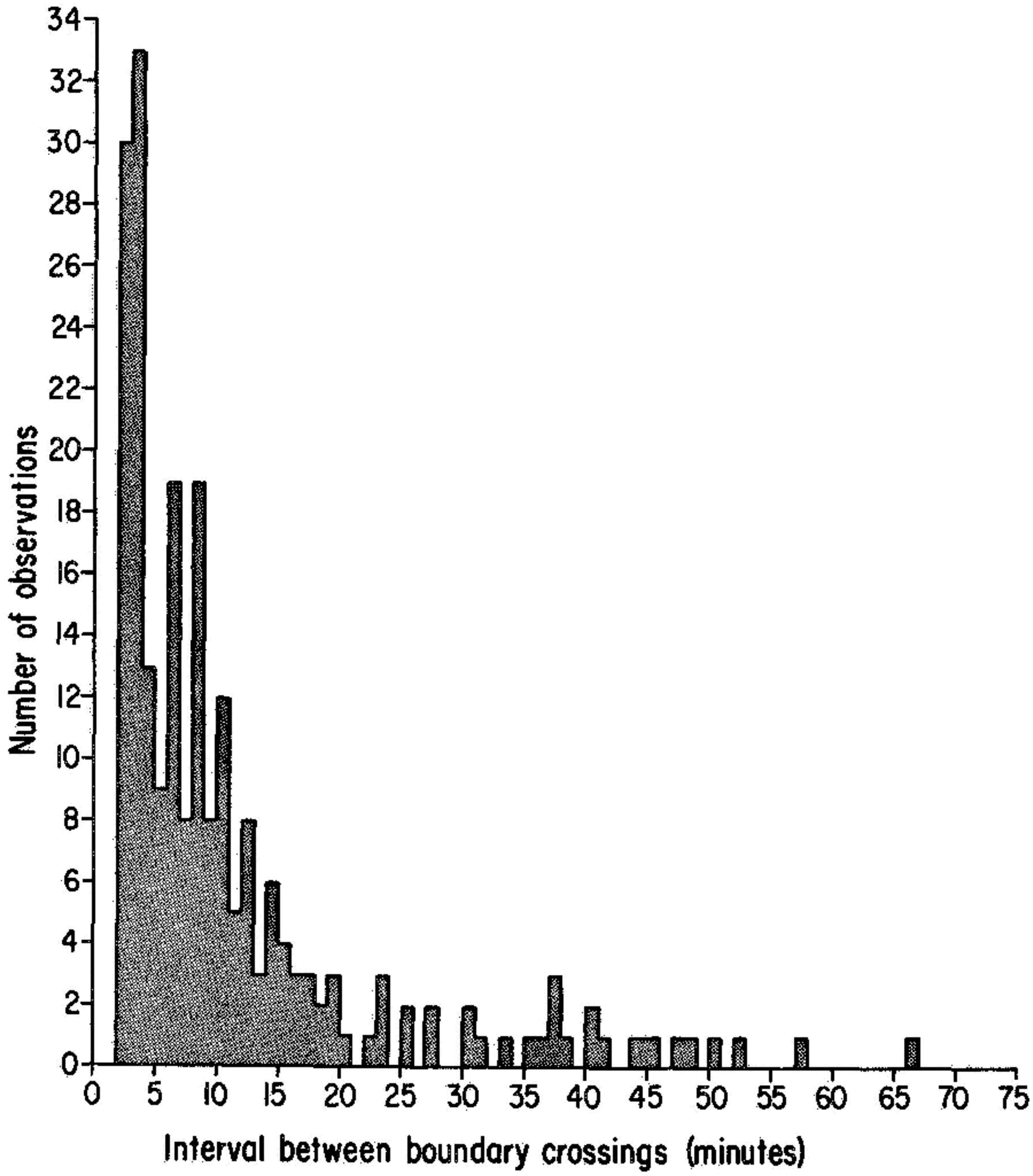
Number of observations
Interval between boundary crossings (minutes)
0 5 10 15 20 25 30 35 40 45 50 55 60 65 70 75
0 2 4 6 8 10 12 14 16 18 20 22 24 26 28 30 32 34

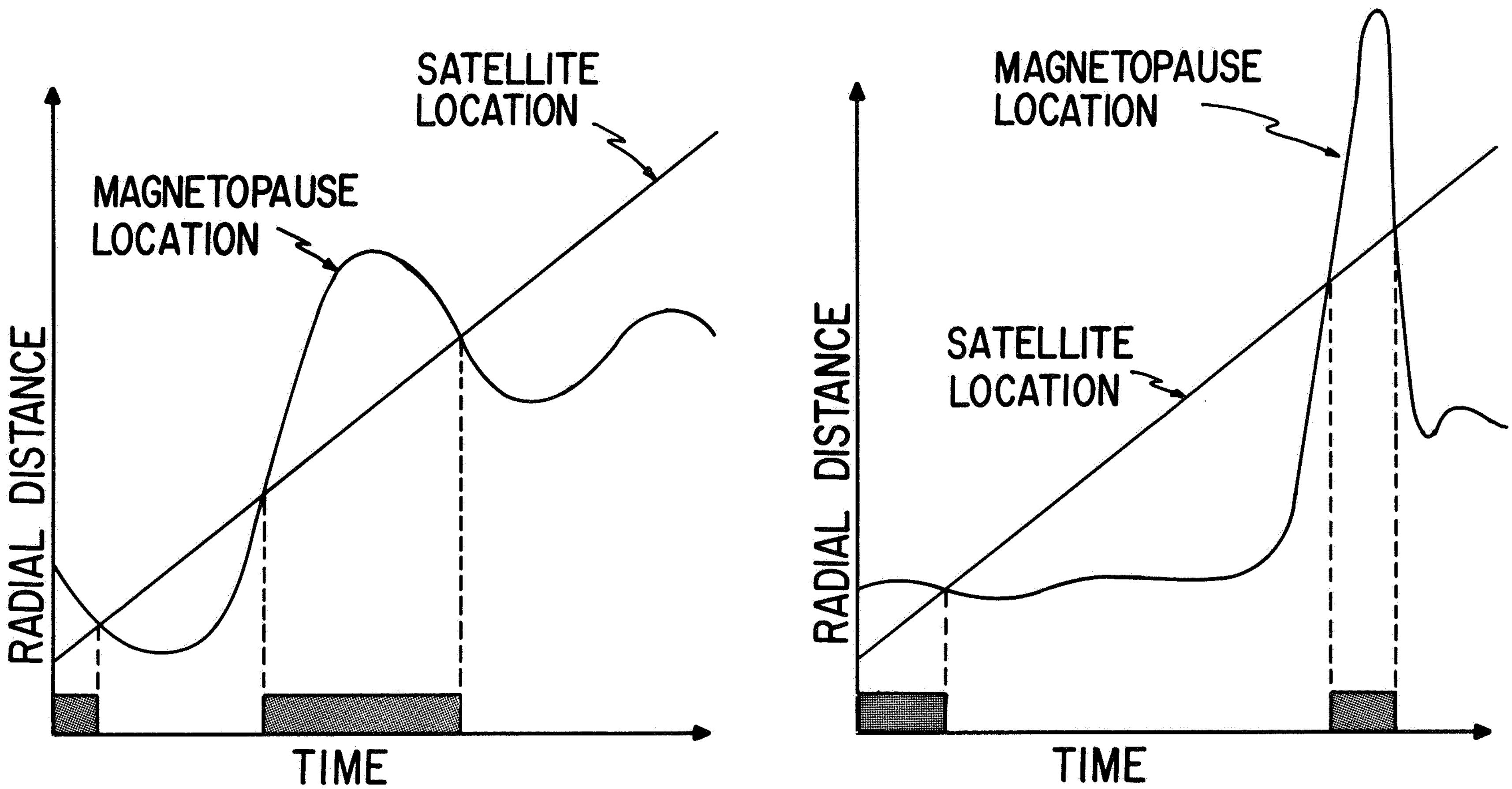
SATELLITE LOCATION
MAGNETOPAUSE LOCATION
RADIAL DISTANCE
TIME
MAGNETOPAUSE LOCATION
SATELLITE LOCATION
RADIAL DISTANCE
TIME

a

b

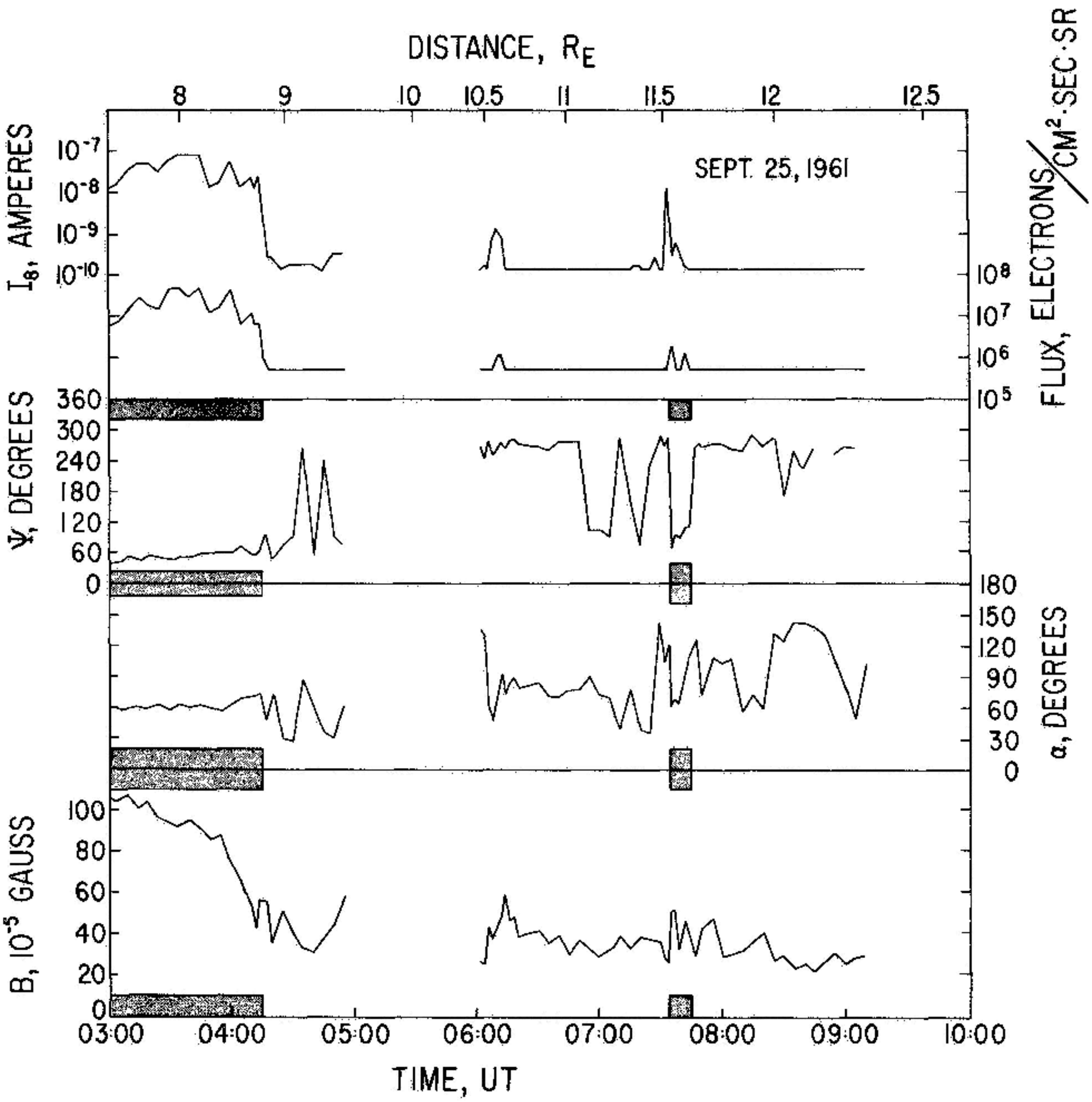

DISTANCE, R_E
8
9
10
10.5
11
11.5
12
12.5
SEPT. 25, 1961
I_8, AMPERES
10^{-7}
10^{-8}
10^{-9}
10^{-10}
FLUX, ELECTRONS/CM²·SEC·SR
10^8
10^7
10^6
10^5
Ψ, DEGREES
360
300
240
180
120
60
0
α, DEGREES
180
150
120
90
60
30
0
B, 10^{-5} GAUSS
100
80
60
40
20
0
03:00
04:00
05:00
06:00
07:00
08:00
09:00
10:00
TIME, UT

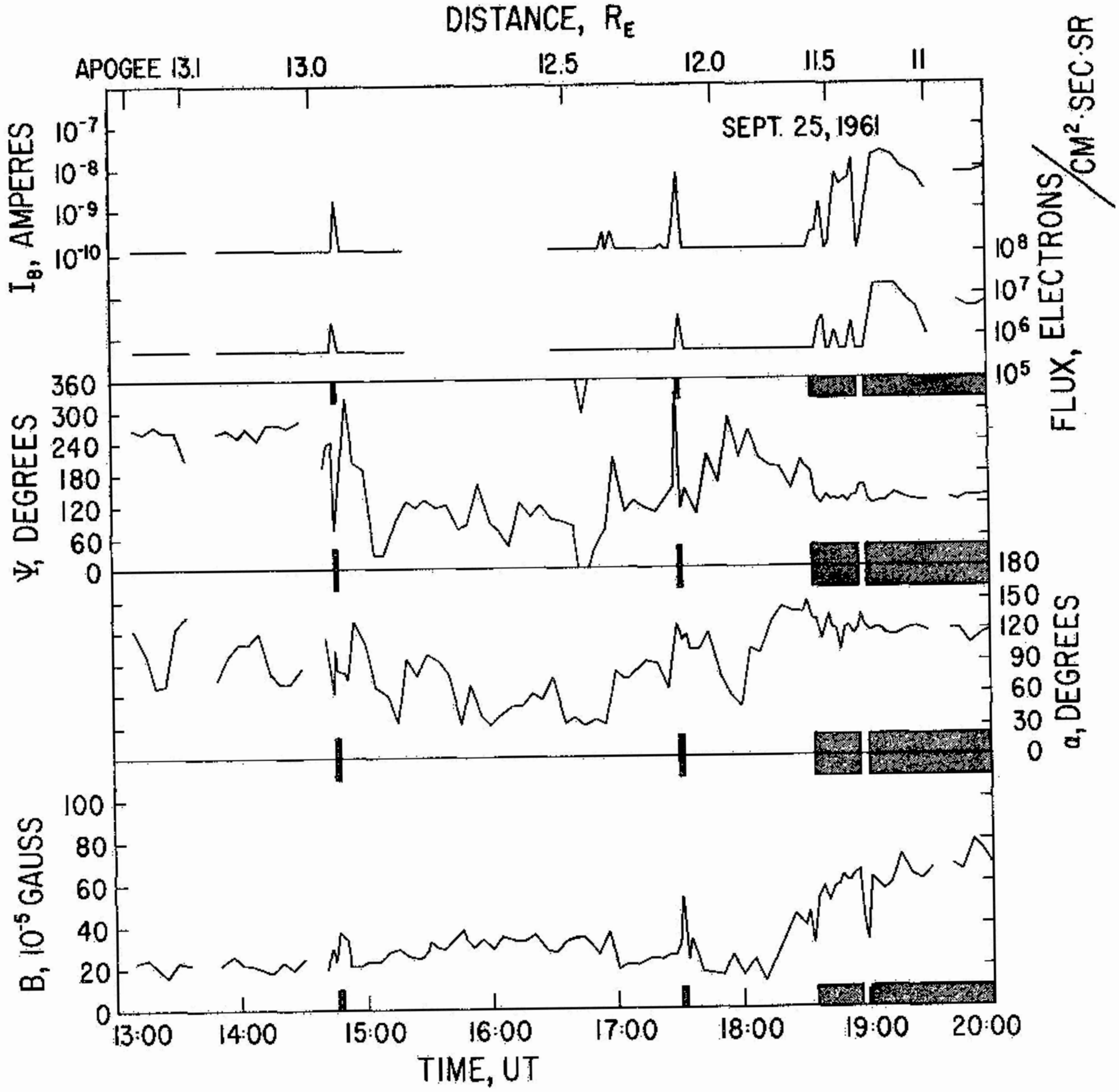
DISTANCE, R_E
APOGEE 13.1
13.0
12.5
12.0
11.5
11
SEPT. 25, 1961
I_B, AMPERES
10^{-7}
10^{-8}
10^{-9}
10^{-10}
FLUX, ELECTRONS/CM²·SEC·SR
10^8
10^7
10^6
10^5
Ψ, DEGREES
360
300
240
180
120
60
0
α, DEGREES
180
150
120
90
60
30
0
B, 10^{-5} GAUSS
100
80
60
40
20
0
13:00
14:00
15:00
16:00
17:00
18:00
19:00
20:00
TIME, UT

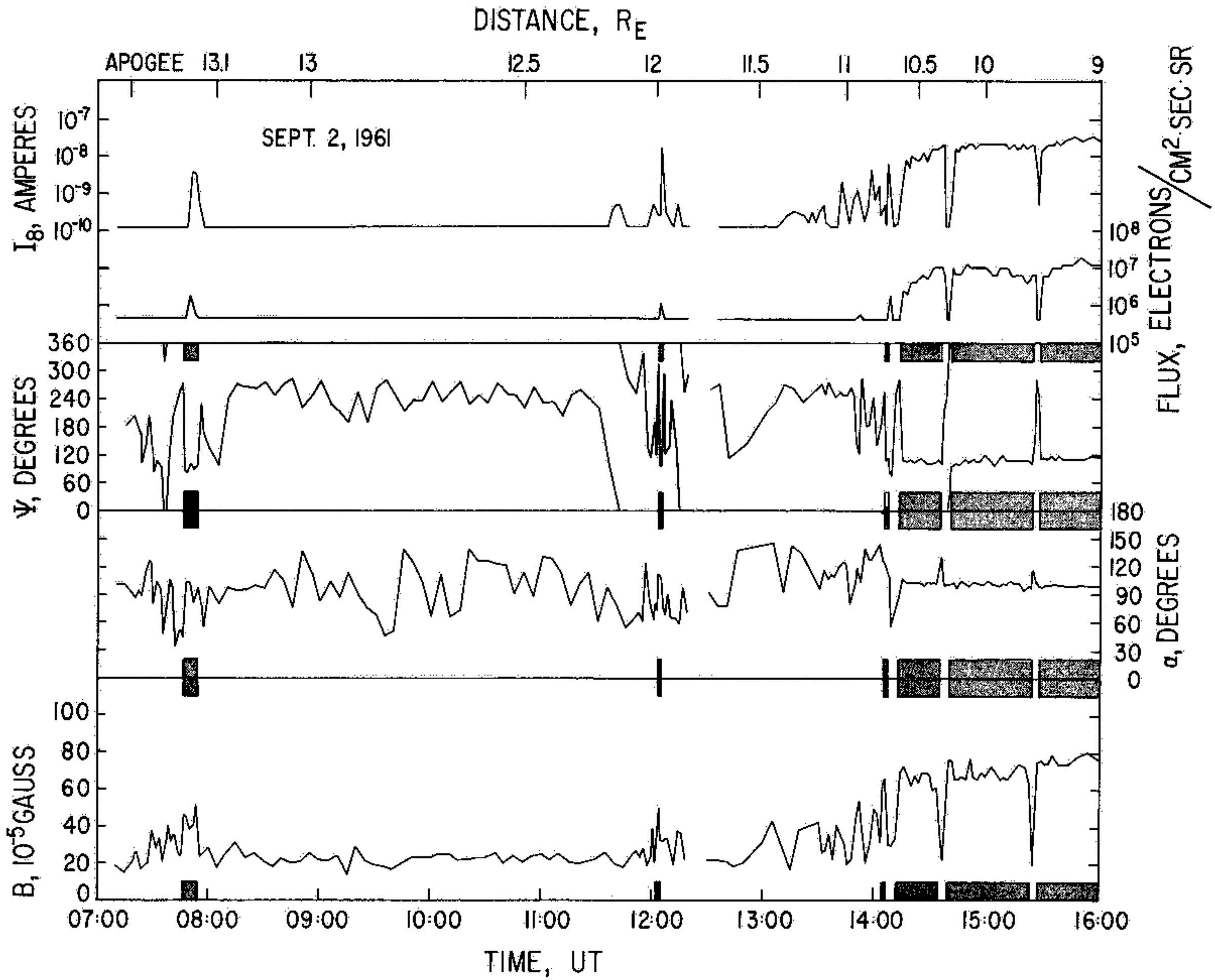
DISTANCE, R_E
APOGEE 13.1
13
12.5
12
11.5
11
10.5
10
9
SEPT. 2, 1961
I_8, AMPERES
10^{-7}
10^{-8}
10^{-9}
10^{-10}
FLUX, ELECTRONS/$CM^2 \cdot SEC \cdot SR$
10^8
10^7
10^6
10^5
Ψ, DEGREES
360
300
240
180
120
60
0
α, DEGREES
180
150
120
90
60
30
0
B, 10^{-5}GAUSS
100
80
60
40
20
0
07:00
08:00
09:00
10:00
11:00
12:00
13:00
14:00
15:00
16:00
TIME, UT

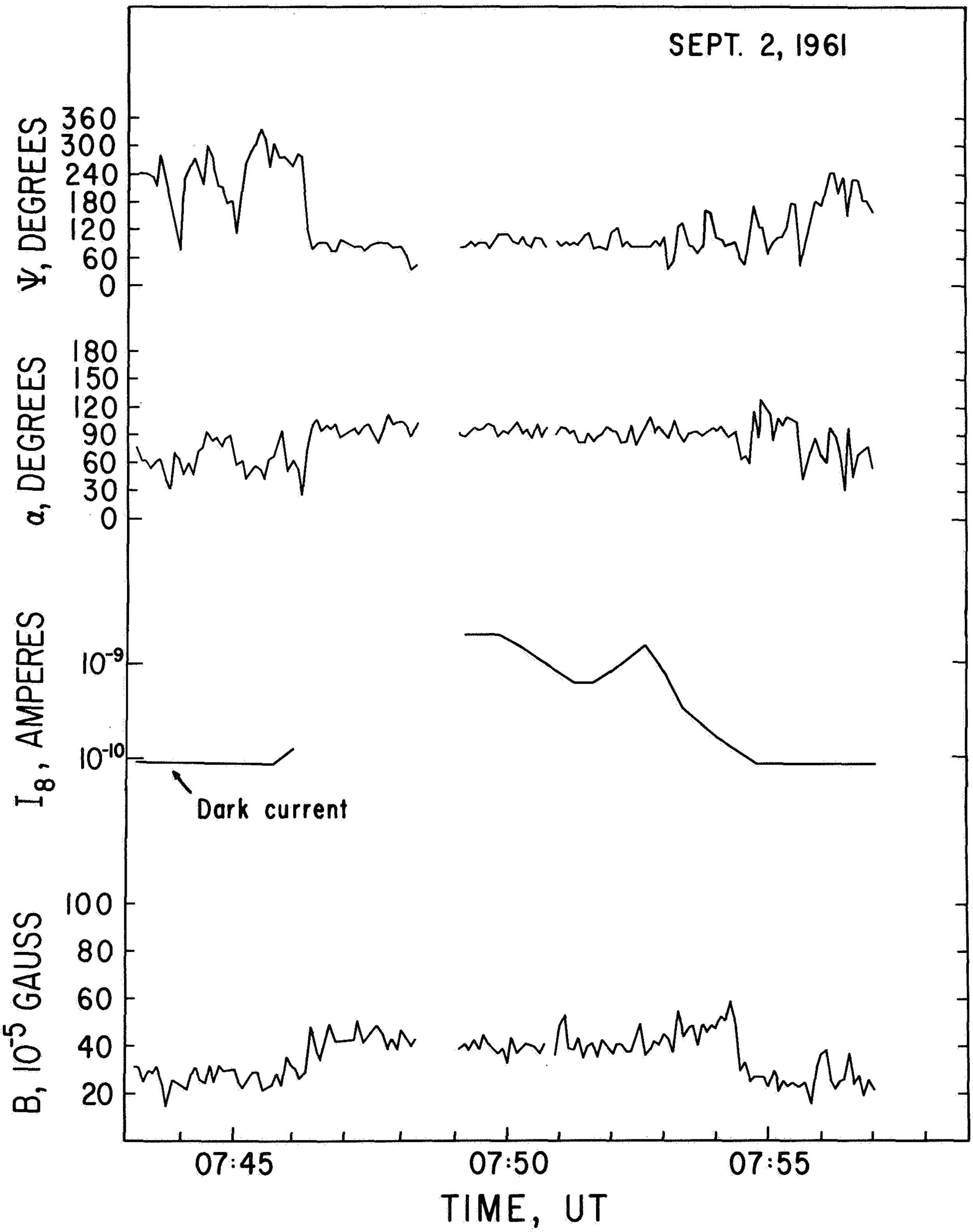
SEPT. 2, 1961
Ψ, DEGREES
360
300
240
180
120
60
0
α, DEGREES
180
150
120
90
60
30
0
I_8, AMPERES
10^{-9}
10^{-10}
Dark current
B, 10^{-5} GAUSS
100
80
60
40
20
07:45
07:50
07:55
TIME, UT

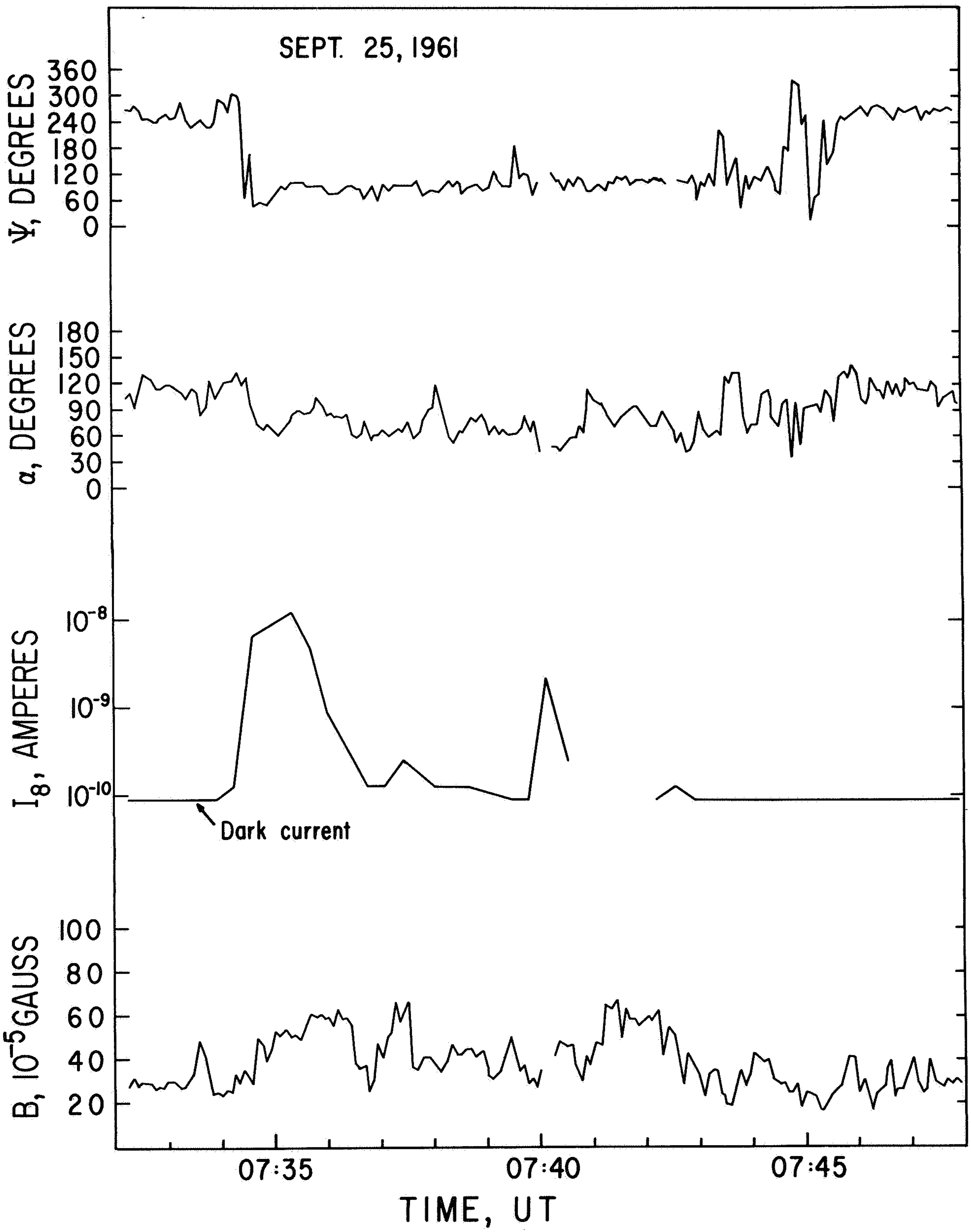

SEPT. 25, 1961
Ψ, DEGREES
360
300
240
180
120
60
0
α, DEGREES
180
150
120
90
60
30
0
I_8, AMPERES
10^{-8}
10^{-9}
10^{-10}
Dark current
B, 10^{-5} GAUSS
100
80
60
40
20
07:35
07:40
07:45
TIME, UT

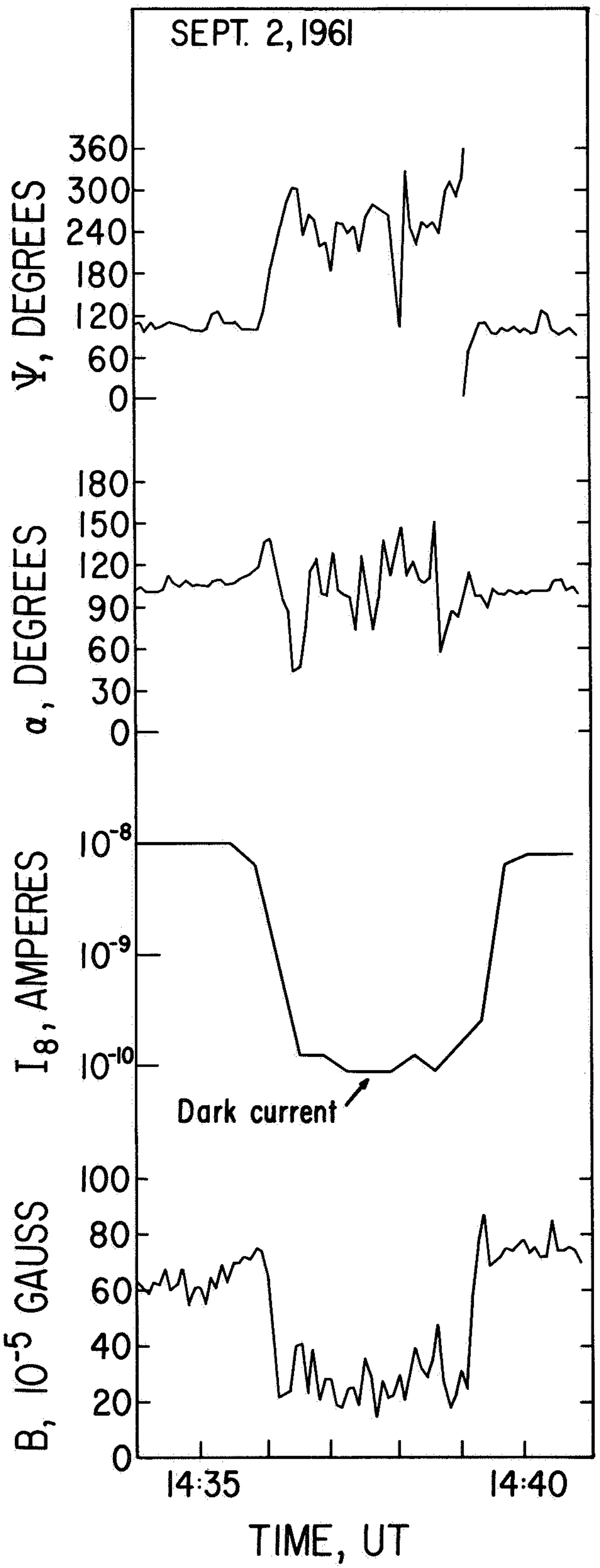

SEPT. 2, 1961
Ψ, DEGREES
360
300
240
180
120
60
0
a, DEGREES
180
150
120
90
60
30
0
I8, AMPERES
10-8
10-9
10-10
Dark current
B, 10-5 GAUSS
100
80
60
40
20
0
14:35
14:40
TIME, UT

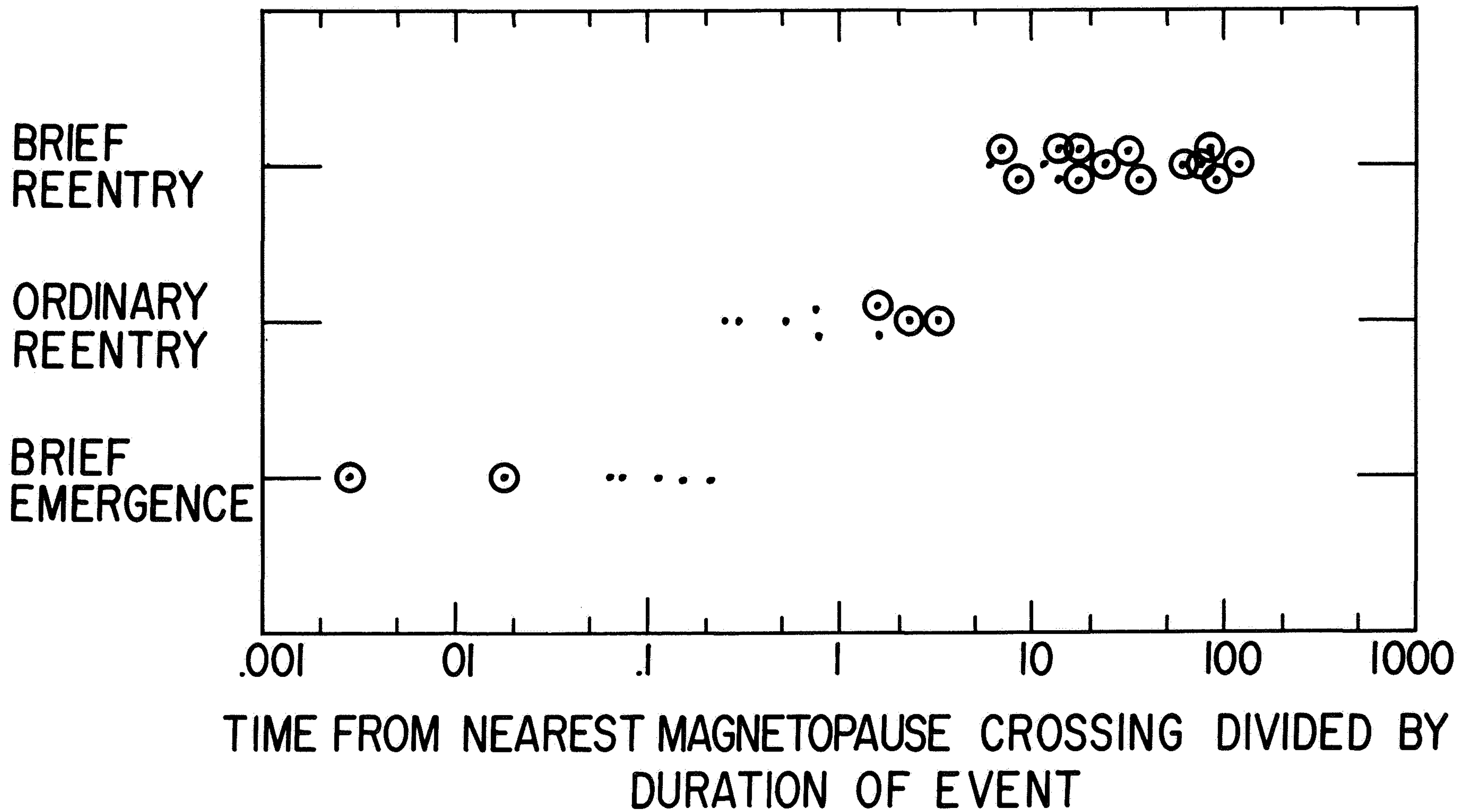

BRIEF REENTRY
ORDINARY REENTRY
BRIEF EMERGENCE
.001
01
.1
1
10
100
1000
TIME FROM NEAREST MAGNETOPAUSE CROSSING DIVIDED BY DURATION OF EVENT

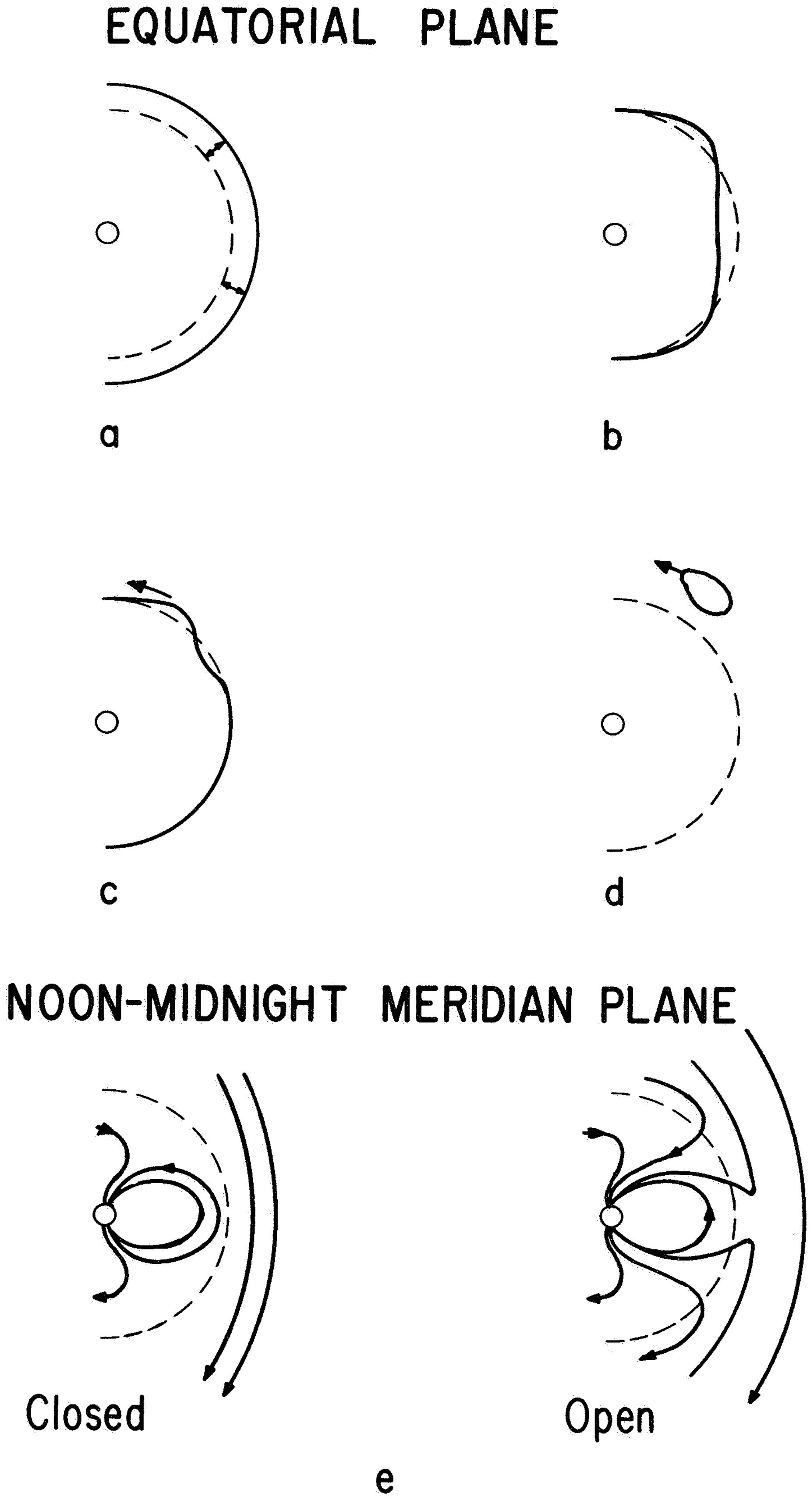
EQUATORIAL PLANE
a
b
c
d
NOON-MIDNIGHT MERIDIAN PLANE
Closed
Open
e

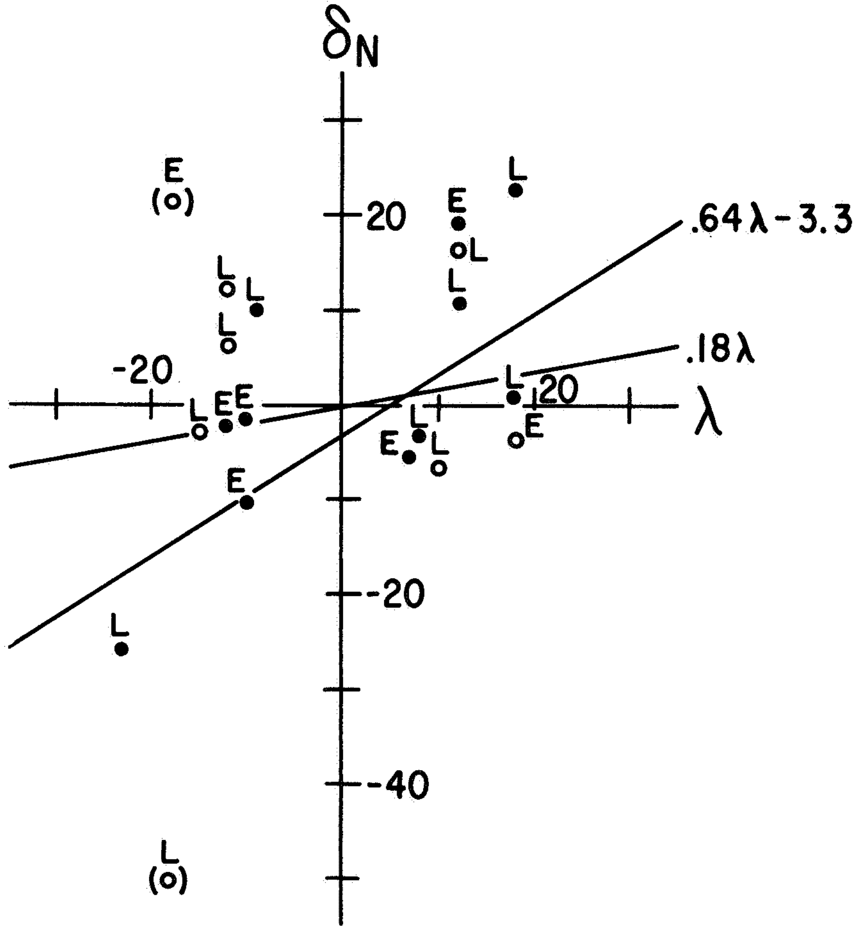

δN
20
-20
-40
-20
20
λ
.64λ-3.3
.18λ
E
L

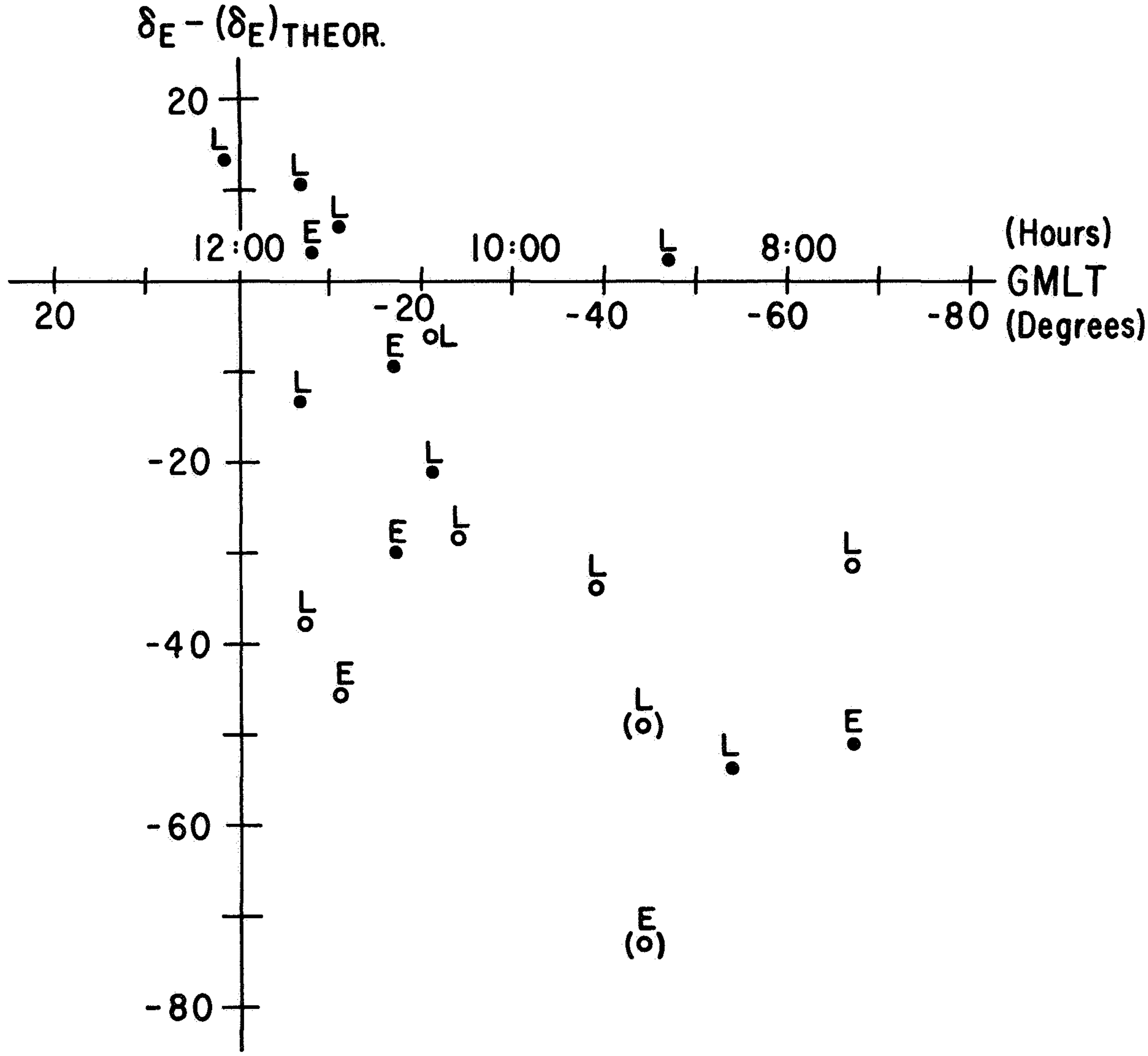

$\delta_E - (\delta_E)_{THEOR.}$
20
-20
-40
-60
-80
12:00
10:00
8:00
(Hours)
GMLT
(Degrees)
20
-20
-40
-60
-80

0956 August 27, 1961

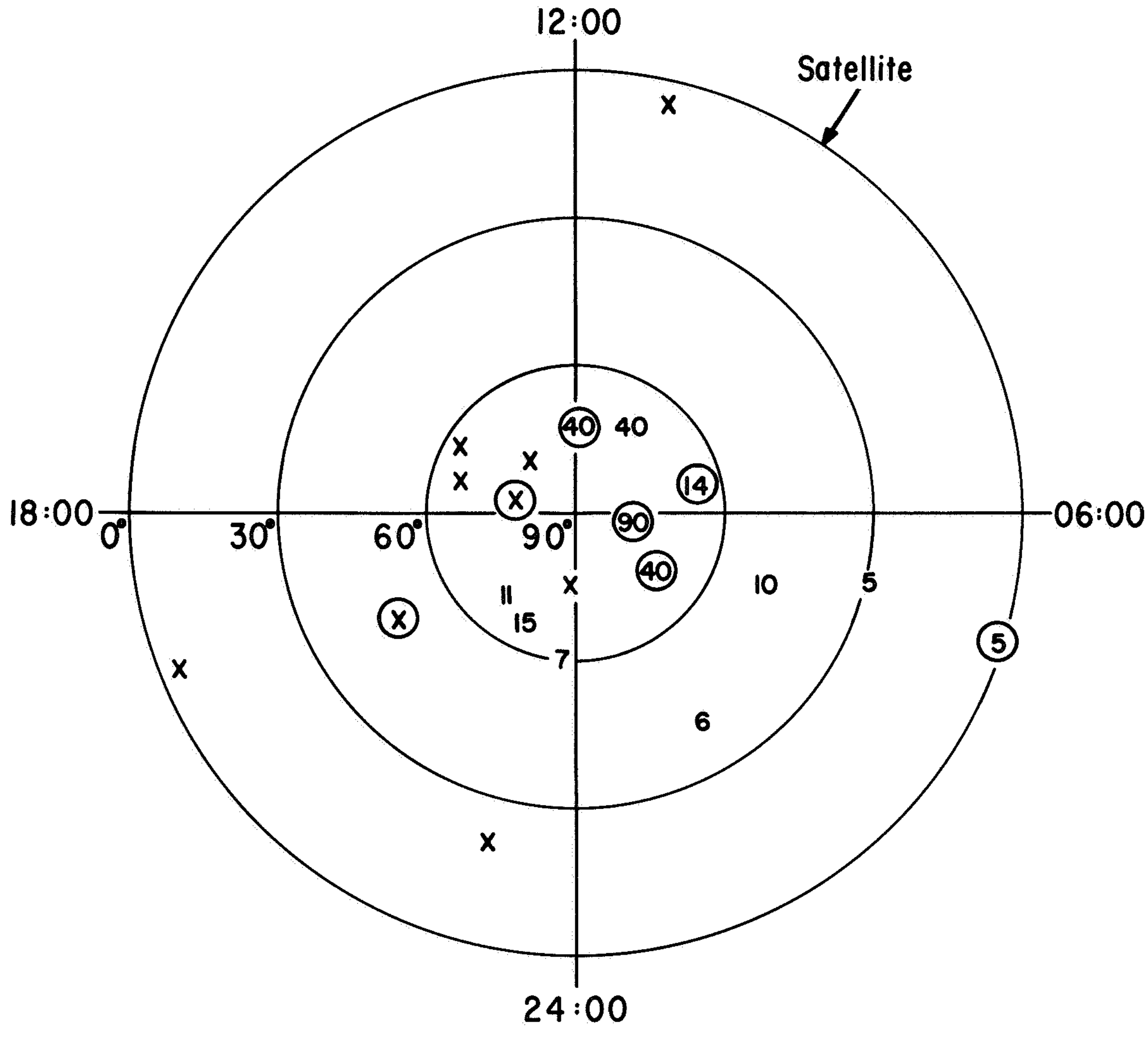

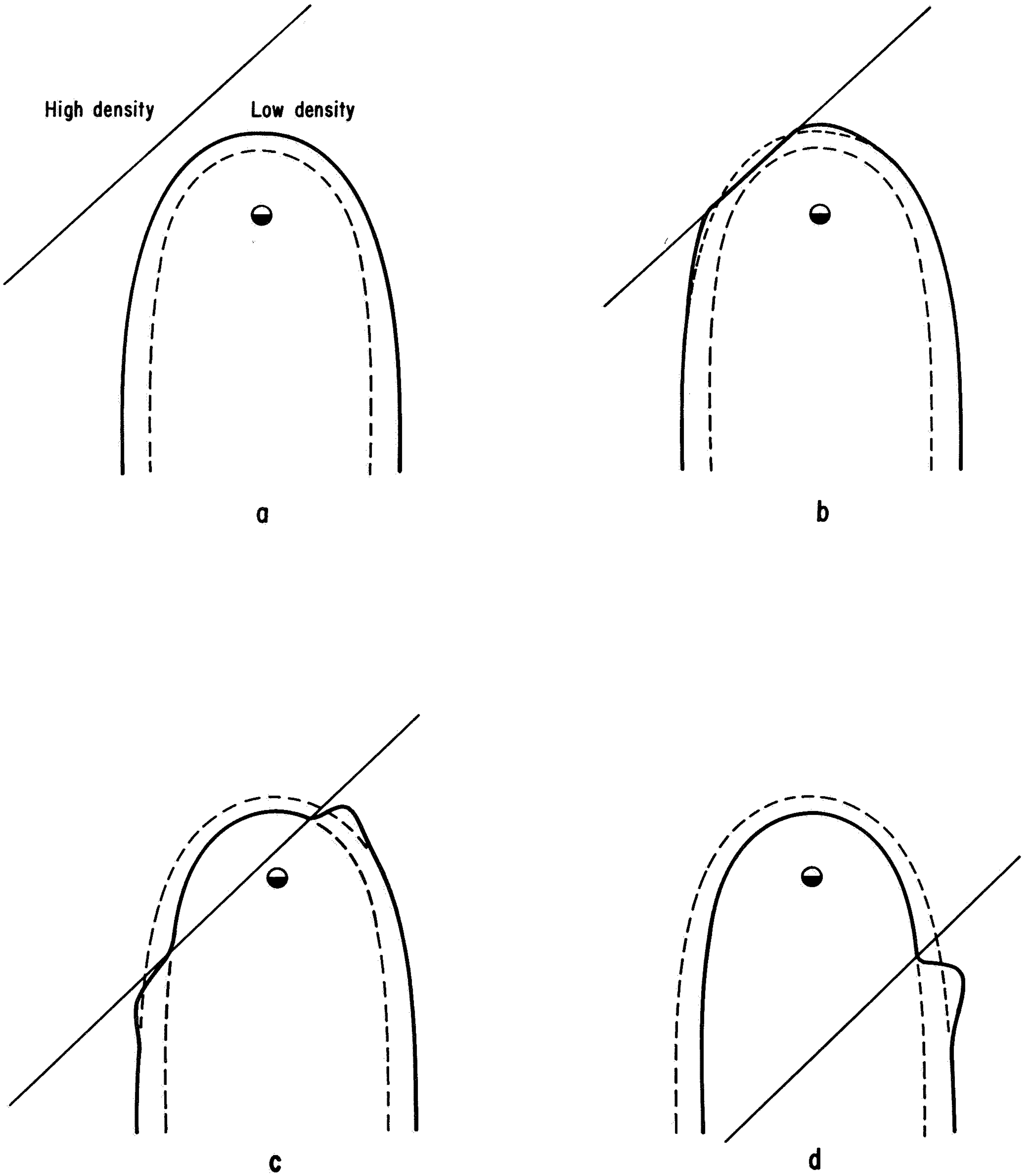
High density
Low density
a
b
c
d

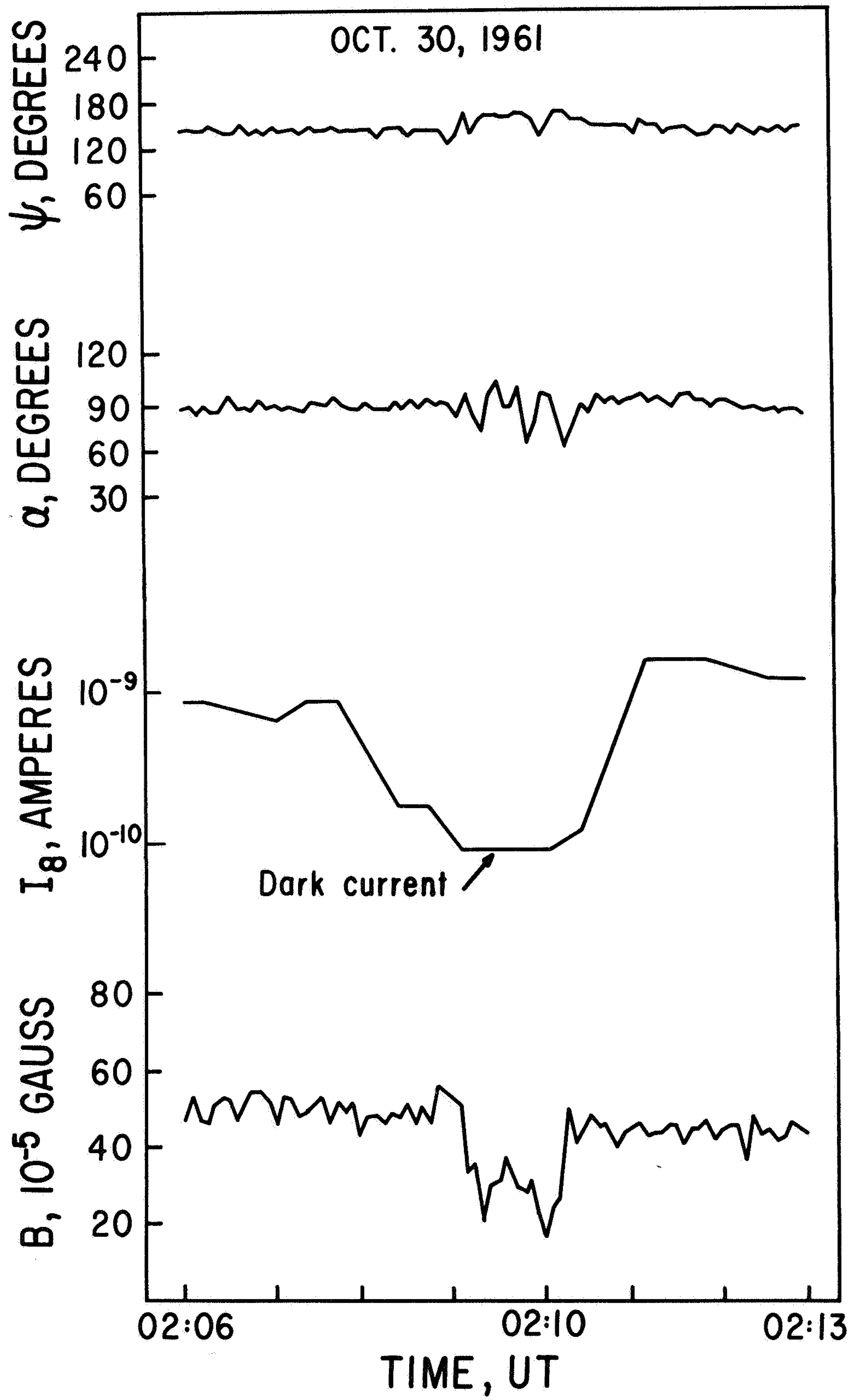

OCT. 30, 1961
ψ, DEGREES
240
180
120
60
α, DEGREES
120
90
60
30
I8, AMPERES
10-9
10-10
Dark current
B, 10-5 GAUSS
80
60
40
20
02:06
02:10
02:13
TIME, UT